FEBS Letters 511 (2002) 150–154 FEBS 25695

DNA intercalation in neutral multilamellar membranes

Tanja Pott[a,b,*], Didier Roux[a]

[a] *Centre de Recherche Paul Pascal – CNRS, Av. A. Schweitzer, 33600 Pessac, France*
[b] *UMR 6052, Ecole Nationale Superieur de Chimie de Rennes, Av. du Général Leclerc, 35700 Rennes Beaulieu, France*

Received 14 September 2001; accepted 31 October 2001

First published online 4 January 2002

Edited by Maurice Montal

Abstract We report a small angle X-ray scattering study of the DNA/neutral lipid/water system showing that it is possible to confine DNA into a neutral multilamellar phase at high lipid-to-DNA weight ratio, despite the lack of electrostatic interactions in this system. This phase is characterized by a 2D ordering of the DNA molecules intercalated between the neutral bilayers of a 3D smectic phase as shown from the presence of a DNA–DNA correlation peak and the 1D electron density profile of the multilamellar phase. We further demonstrate that it is possible to disperse this phase as small multilamellar vesicles encapsulating high amounts of DNA.

Key words: DNA; Encapsulation; Multilamellar vesicle; Phospholipid; Diacylglycerophosphatidylcholine; X-ray diffraction

1. Introduction

Gene delivery methods, designed to introduce genetic material into patients' cells, usually employ a DNA carrier, the so-called vector. Recombinant viral vectors are commonly utilized, yet safety concerns as well as the problem of large-scale production set a limit to their usefulness [1] and prompted the surge of research on non-viral synthetic vector systems [2]. During the last decade there has been a tremendous activity in the development of DNA delivery systems held together by electrostatic interactions between the negatively charged nucleic acids and a cationic vector. In particular complexes based on cationic lipids (CLs) have become the most fashionable of all the easy-to-prepare, synthetic vectors. Since the pioneering work of Felgner et al. [3,4] it has been well established that CL–DNA complexes with an overall positive charge enhance transfection by attaching easily to anionic animal cell membranes. Numerous CLs with monovalent or polyvalent headgroups have been described subsequently and different structural arrangements have been reported [3,5–7]. Recently it has been shown that CL–DNA complexes have ordered liquid-crystalline structure and their precise topology has been proved to be defined by the helper lipid [8,9]. In the case of a typical bilayer-forming helper lipid, dioleylphosphatidylcholine (DOPC), lamellar complexes with the DNA intercalated between the lipid bilayers (L_α^c) are obtained [9].

One of the main problems when using CL formulations is their inherent toxicity [10–13]. Yet, neutral or negatively charged liposomes known to be of lower toxicity than CL appear inconvenient as DNA vectors, as they lack electrostatic interactions with the DNA so that encapsulation ratios are typically negligible. Recently, a process to prepare small multilamellar vesicles (sMLV) by shearing of a concentrated L_α phase has been proposed [14]. Herein we used this process to encapsulate high amounts of DNA in sMLV using neutral lipids only (NLs).

2. Materials and methods

Pure soya bean diacylphosphatidylcholine (PC) was obtained from Avanti Polar Lipids, 1-monoolein (MO) from Sigma, France and C12E4 from Seppic. The NL mixtures were prepared by cosolubilization from methanol. After evaporation of the solvent the lipid film was desiccated under vacuum overnight, redispersed in Millipore water and freeze-dried. For all experiments shown herein a PC-to-helper surfactant weight ratio of 95:5 was utilized. Short DNA fragments were obtained by sonication of highly polymerized bovine thymus DNA (Sigma, France). The size of DNA fragments was verified by gel electrophoresis to be around 150 bp ($\sim$500 Å). Control experiments on dilute samples were carried out using pCMV luciferase plasmid (5581 bp) obtained from Qiagen, Germany. NL–DNA mixtures were prepared by mixing lipids and DNA at a given NL-to-DNA weight ratio, ρ, in excess water followed by freeze-drying. The obtained dry powder was then hydrated with the appropriate amount of deionized water. The SAXS (small angle X-ray scattering) experiments were carried out on the beamline ID02A at the European Synchrotron Research Facility (ESRF, Grenoble, France) or at the laboratory using a rotating anode X-ray generator. YOYO-1 iodide was obtained from Molecular Probes and used to determine the percentage of encapsulated DNA by fluorescence spectroscopy (λ_{ex} = 491 nm, λ_{em} = 509 nm). It was verified that the increase in fluorescence was linearly proportional to the amount of DNA in the concentrations used herein. All fluorescence measurements were made at least twice and averaged.

3. Results and discussion

PC was chosen as neutral and natural phospholipid (PCs are actually zwitterionic bearing a very weak negative overall charge when organized in a bilayer [15]). To facilitate shear-induced sMLV formation [14] a small amount of a neutral helper surfactant was added. Two helper surfactants were investigated, MO bearing a negative spontaneous curvature and dodecyltetraoxoethylene (C12E4) characterized by a positive spontaneous curvature. The influence of the nature of the

*Corresponding author. Fax: (33)-2-99 87 13 98.
E-mail address: tanja.pott@ensc-rennes.fr (T. Pott).

Abbreviations: CL, cationic lipids; NL, neutral lipids; ρ, lipid-to-DNA weight ratio; ρ*, NL-to-encapsulated DNA weight ratio; SAXS, small angle X-ray scattering; sMLV, small multilamellar vesicles; $sMLV_{DNA}$, DNA-containing small multilamellar vesicles

PII: S0014-5793(01)03315-4

neutral helper surfactant was investigated and was found to be negligible. Experiments were carried out, if not mentioned otherwise, with short DNA fragments (~150 bp) as model DNA. These fragments have a length of ~500 Å corresponding to the persistence length of DNA [16].

The phase diagram of the ternary NL–DNA–water system shows that it is possible to obtain a homogeneous DNA-containing lamellar phase only for quite high amounts of DNA (Fig. 1A). Synchrotron SAXS scans of this phase as a function of NL-to-DNA weight ratio, ρ, at fixed $\Phi_{H_2O} = 0.5$ (Φ_{H_2O} is the weight fraction of water) are shown in Fig. 1B. In the absence of DNA ($\rho = \infty$) five sharp Bragg reflections of a lamellar phase with a repeat distance, d, of 62.8 Å are observed, a value commonly found for a fully swollen L_α phase of PC multilayers. The SAXS scans obtained for the DNA-containing lamellar phase give rise to several sharp peaks (six to eight orders) indicative of a single lamellar lattice, but differ from the DNA-free system by two distinct features. First, there is a quite large increase in the repeat distance of the lamellar lattice leading to 75.8 Å at $\rho = 4$. For higher DNA amounts (smaller ρ) the repeat distance varies little. Second, a broad peak at $q = 0.16$–0.21 increasing in intensity as ρ decreases is detected (Fig. 1C, arrows). This peak can be attributed to DNA–DNA correlation and relates

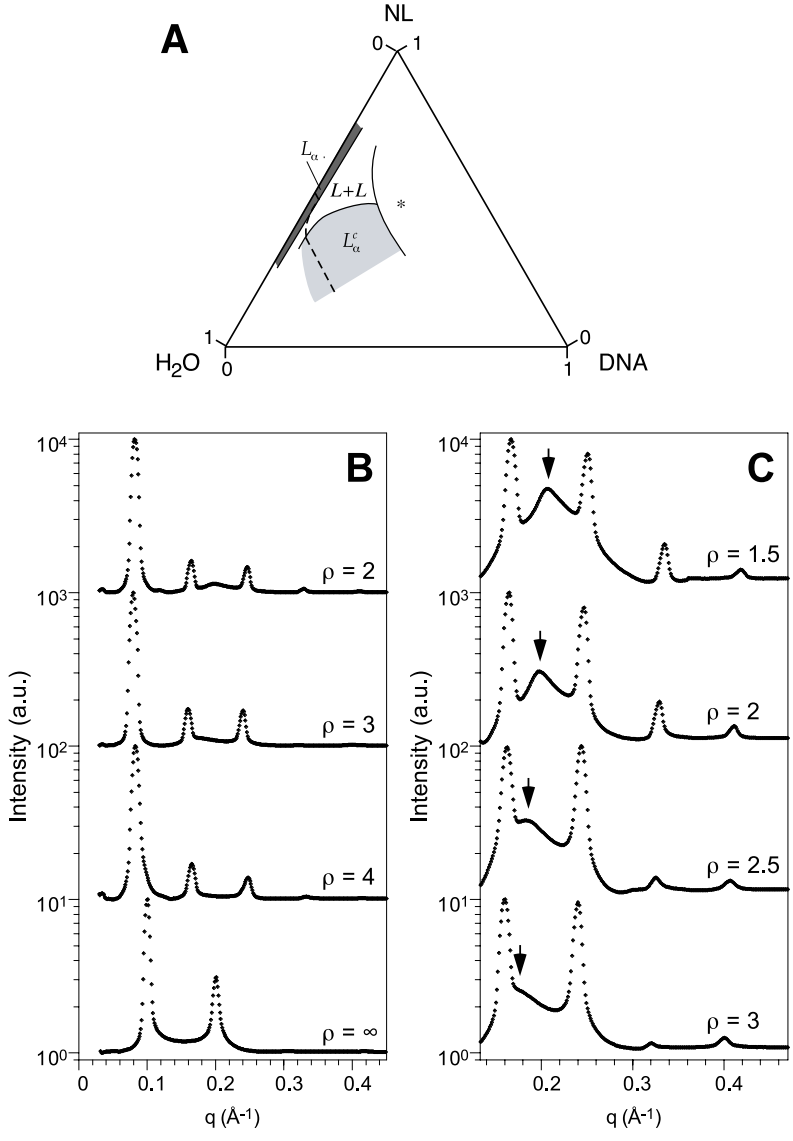

Fig. 1. A: Schematic presentation of the partial phase diagram obtained from SAXS data. The asterisk denotes a region in the phase diagram where samples are inhomogeneous and do not reach equilibrium on a reasonable timescale. The dashed line indicates the swelling limit where the different lamellar phases coexist with excess aqueous phase. B: Selected synchrotron SAXS scans of NL–DNA lamellar phases (L^c_α phase) at fixed $\Phi_{H_2O} = 0.5$ for different NL-to-DNA weight ratios (ρ) and in the absence of DNA. The L_α phase of the DNA-free NL system ($\rho = \infty$) gives rise to 5 Bragg reflections but only the dominant first two orders at $q_{001} = 0.100$ and $q_{002} = 0.200$ can be distinguished in this representation. For the DNA containing systems the observed six to eight orders result from the lamellar L^c_α structure with alternating DNA monolayer and lipid bilayers, the first three orders at $q_{001} = 0.083$, $q_{002} = 0.166$ and $q_{003} = 0.248$ ($\rho = 4$) can easily be recognized. The increase in the DNA content of the L^c_α phase results further in the appearance of a broad peak around $q \approx 0.2$ that is due to the correlation between DNA molecules. C: Parts of a series of synchrotron SAXS scans of the NL–DNA L^c_α phase ($\Phi_{H_2O} = 0.5$) focussing on the broad diffraction peak at q_{DNA} (arrow) due to the DNA interaxial spacing d_{DNA} (see also Fig. 2C) as a function of ρ; of the lamellar spacing only the second to fifth orders are shown.

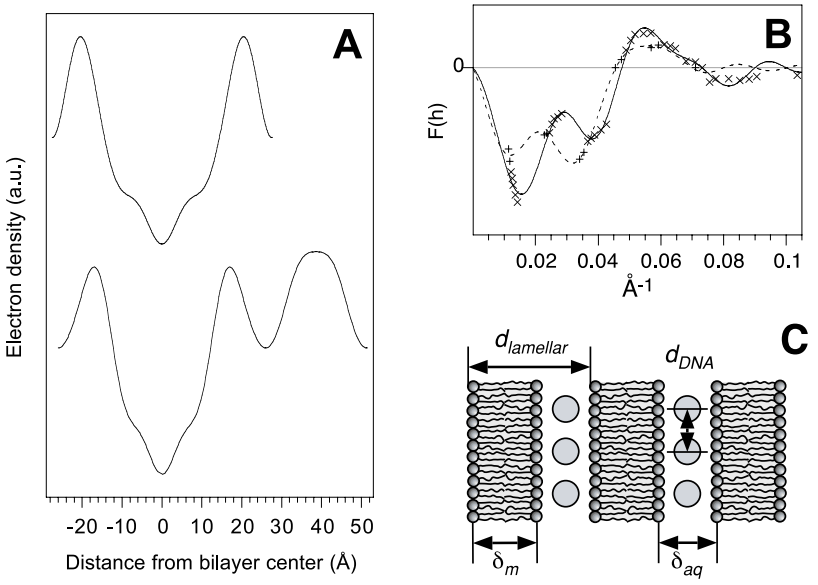

Fig. 2. A: Electron density profile of the NL–DNA L_α^c phase at $\rho = 2$ and $\Phi_{H_2O} = 0.5$ reconstructed from eight orders of the lamellar reflections (bottom) as a function of the distance from the bilayer center. For comparison the electron density profile of the L_α phase of a pure PC is also shown (top). In both cases one repeat unit is shown. It can be noted that the NL bilayer is with $\delta_m \approx 34$ Å thinner than the $\delta_m \approx 40$ Å obtained for the pure PC. This is as expected when comparing a synthetic PC with a natural extract containing a single chain surfactant. B: Amplitudes of the swelling series of the NL–DNA L_α^c phase at $\rho = 2$. Note that the swelling series is best represented by two continuous transforms, one for samples in the swelling regimes at constant DNA content, the other for samples having excess aqueous phase. Assuming that in the latter case the DNA concentrations in the interstitial and the excess aqueous phase are identical, the DNA content in the L_α^c should decrease, resulting in a change in the exact structure of the L_α^c phase that should indeed lead to a break in the smooth curve. Then the data sample a set of similar continuous transforms. C: Schematic representation of the NL–DNA L_α^c phase showing the different parameters defining the local arrangement of this phase. The DNA molecules can be represented as rods viewed from the top in this presentation.

to the DNA interaxial spacing by $d_{DNA} = 2\pi/q_{DNA}$ (see also Fig. 2C). It can further be noted that the peak is shifted towards higher q_{DNA} (smaller d_{DNA}) as ρ decreases. Both features, the increase in d and the appearance of q_{DNA}, are in agreement with a multilamellar L_α structure with intercalated monolayer DNA between the neutral lipid bilayers. Indeed the diffraction patterns are surprisingly similar to the one of the L_α^c phase found for CL–DNA complexes [9]. Nevertheless in the absence of electrostatic interactions the DNA is confined into the interstitial space rather than condensed by a counterion mechanism (so herein the 'c' in L_α^c phase should be understood as *confined*, not condensed).

We further reconstructed the 1D electron density profile of the structure taking into account the lamellar reflections only (Fig. 2A). Intensities from the peaks in the synchrotron SAXS scans from powder samples were obtained by integration after background subtraction and corrected for the Lorentz factor. The swelling method was used for the determination of the relative phases of Bragg reflection [17] and intensities were scaled to satisfy Blaurock's scaling relation [18]. Amplitudes, i.e. the square root of the scaled intensities ($F(h) = \sqrt{I(h)}$), are plotted in Fig. 2B as a function of the reciprocal lattice vector ($4\pi\sin\theta/\lambda$) for the NL–DNA system at $\rho = 2$. The phases of the centrosymmetric structure were chosen so that the data points fall on a single smooth curve. Alternative phase assignments for higher orders were considered and rejected as they produced electron density profiles that were physically implausible. Fig. 2A shows the resulting electron density profile of the NL–DNA system at $\rho = 2$ and $\Phi_{H_2O} = 0.5$ (bottom) and the one of a pure PC L_α phase (top) for comparison. The electron density profiles of the bilayer parts are qualitatively identical. More important, for the NL–DNA system one notices a huge broad bulge in the electron density centered at about 38 Å from the bilayer center due to the presence of high amounts of DNA in the interstitial space. This is in full agreement with the idea of a L_α^c phase formed by the NL–DNA system. Besides, from the electron density profiles it could be deduced that $\delta_m \approx 34$ Å (δ_m is taken herein as HTH distance,

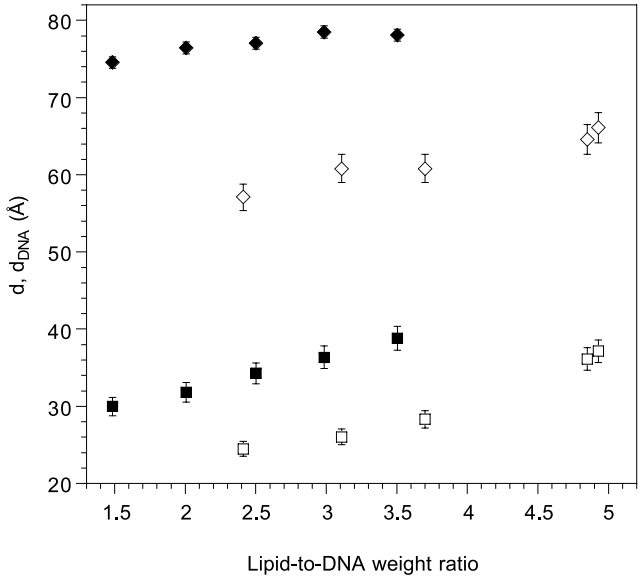

Fig. 3. DNA interaxial spacing d_{DNA} (■) and lamellar spacing d (♦) as a function of the lipid-to-DNA weight ratios, ρ, determined from the synchrotron SAXS scans of NL–DNA lamellar phases at $\Phi_{H_2O} = 0.5$. For comparison d_{DNA} (□) and d (◇) of the L_α^c phase of CL–DNA complexes (DOTAP/DNA = 2.4 with DOPC as helper lipid) are also shown (data taken from Fig. 4 in [9]).

i.e. head-to-head, or better phosphate-to-phosphate distance, measured directly from the electron density profile; see also Fig. 2C) does not vary either with hydration or with DNA content of the system. This demonstrates nicely that the DNA in this system, in contrast to CL–DNA complexes, does not interact strongly with the lipid bilayers.

From a thermodynamic point of view the L_α^c phase of NL–DNA systems is actually closer to the 'doped-solvent' lamellar phases [19] than to the L_α^c phase of CL–DNA complexes [9] as there are no favorable interactions between the NLs and the DNA. Consequently the NL–DNA system does not self-assemble in excess water and the concentrated state is needed to confine the DNA into the interstitial space. The only difference with the ordinary 'doped-solvent' lamellar phase is the liquid-crystalline state of the DNA molecules confined to the interstitial space. To our knowledge this is the first time that such a phase has been described.

When comparing d and d_{DNA} of DNA-containing NL and the CL systems (Fig. 3), it can be seen that although qualitatively similar d and d_{DNA} of NL and CLs differ in their absolute value. Both d and d_{DNA} of the NL system are larger than those of the CL complexes. In the case of the CL L_α^c phase δ_{aq} (δ_{aq} is the thickness of the aqueous DNA-containing layer, see also Fig. 2C) is only 25 ± 1.5 Å which equals the minimum d_{DNA} found in this system [9]. With δ_{aq} about 40–44 Å (δ_{aq} was determined by $\delta_{aq} = d - \delta_m$ with $\delta_m = 34$ Å) in the NL L_α^c phase, δ_{aq} is not only considerably larger than in the CL–DNA complexes but also always larger than d_{DNA} of the NL–DNA system. It seems likely that the DNA molecules in the NL L_α^c phase have substantially more motional freedom than in the CL systems, which may account for the greater d_{DNA} found in the NL L_α^c phase at equal ρ.

Due to the small quantities of the NL–DNA system and its high viscosity the use of a couette was not possible, sMLV

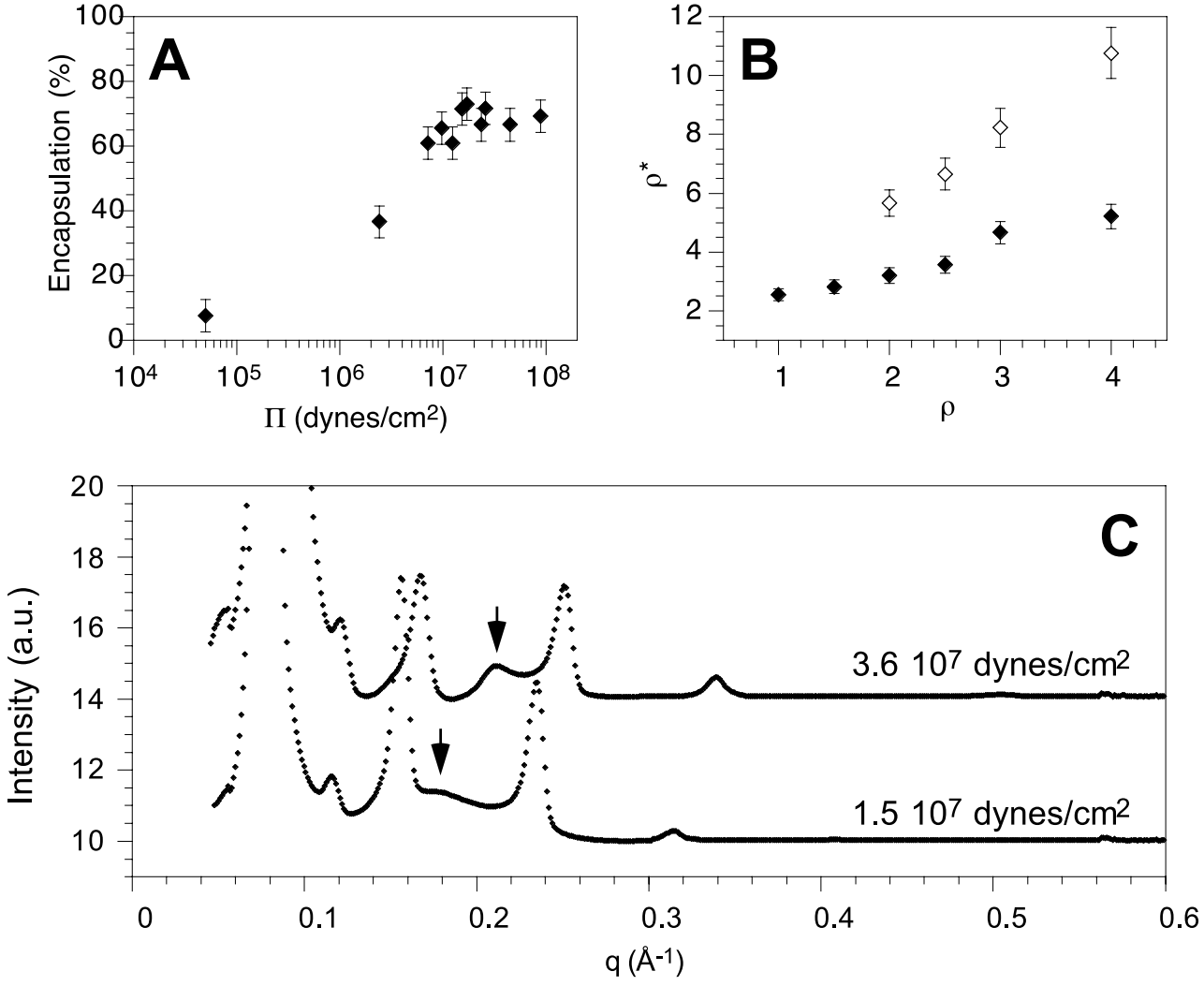

Fig. 4. A: Encapsulation of DNA as a function of the osmotic pressure Π of the buffer used to disperse the $sMLV_{DNA}$ prepared from the NL–DNA L_α^c phase ($\rho = 2$) by inhomogeneous shearing. Π of an aqueous DNA solution corresponding to the DNA concentration of the interstitial space was measured to be 1.3×10^7 dynes/cm^2. Π of the Tris buffer system (pH 7.4) was adjusted with NaCl. B: NL-to-encapsulated DNA weight ratio, ρ^*, of the $sMLV_{DNA}$ as a function of the NL-to-DNA weight ratio of the L_α^c phase ρ for short DNA fragments (♦) and the plasmid luciferase (◇). sMLV were dispersed first in a hyperosmotic buffer (2.2×10^7 dynes/cm^2) and the amount of encapsulated DNA was then determined by dilution into a buffer of physiological osmotic pressure ($\sim 7.4 \times 10^6$ dynes/cm^2). C: SAXS scans of $sMLV_{DNA}$ prepared from the NL–DNA L_α^c phase at $\rho = 2$ after elimination of the non-encapsulated DNA at two different Π values. The broad diffraction peak at q_{DNA} due to the DNA interaxial spacing d_{DNA} is indicated by an arrow. The weak diffraction at $q_{001} = 0.11$–0.12 corresponds to a first order of DNA-free multilayers.

were thus prepared by manual shear between two glass plates and the result checked under the microscope using crossed polarizers. The inhomogeneous shear produces polydisperse sMLV (approximately 0.2–1 μm). To disperse the $sMLV_{DNA}$ ($sMLV_{DNA}$ stands for sMLV obtained from the NL L_α^c phase) the osmotic pressure Π arising from the DNA–water layer of the NL L_α^c phase has to be taken into account (Fig. 4A). Indeed, the percentage of encapsulated DNA increases with increasing Π of the buffer and at 70% reaches a maximum at about 1.7×10^7 dynes/cm^2. For higher Π the percentage of encapsulated DNA stays about constant. A fancy behavior of the system is the fact that once the $sMLV_{DNA}$ are dispersed they can be diluted into a buffer of lower Π without apparent leakage of encapsulated DNA. This observation was used subsequently in the dilution of $sMLV_{DNA}$, that is the $sMLV_{DNA}$ were first dispersed in a hyperosmotic buffer and the yield of DNA encapsulation determined upon dilution of the sMLV into a buffer of physiological Π ($\sim7.4\times10^6$ dynes/cm^2). Fig. 4B shows the NL-to-encapsulated DNA weight ratio ρ^* of the $sMLV_{DNA}$ as a function of the ρ of the NL L_α^c phase using either the short DNA fragments or the pCMV plasmid. In both cases ρ^* of the $sMLV_{DNA}$ decreases continuously with decreasing ρ resulting in $sMLV_{DNA}$ characterized by lipid-to-encapsulated DNA weight ratios of two to three for the DNA fragments and about six for the pCMV plasmid. The latter validates the approach adopted herein, i.e. the use of short DNA fragments as a model system.

The question arises whether or not the structure of the L_α^c phase is conserved in the $sMLV_{DNA}$. Fig. 4C shows synchrotron SAXS scans obtained from $sMLV_{DNA}$ obtained from a L_α^c phase at $\rho=2$ and dispersed in two buffers at $\Pi=1.5\times10^7$ dynes/cm^2 and 3.6×10^7 dynes/cm^2 in the range where the yield of encapsulation is maximal and constant (Fig. 4A). It can clearly be seen that the peak at q_{DNA} (arrows) is still present, confirming the integrity of the L_α^c phase in the $sMLV_{DNA}$.

To our knowledge this is the first time a vector based on neutral lipids was found to encapsulate DNA at these huge amounts. We believe that the present study offers new perspectives to DNA vectorization, as it shows that steric confinement can be an extremely efficient method for DNA encapsulation.

Acknowledgements: We thank O. Diat and P. Méléard for discussion and help in the synchrotron measurements. The synchrotron measurements were carried out at ESRF (Grenoble, France) supported by the European community. I. Salesse and V. Metrot are acknowledged for their help in fluorescence measurements. T.P. acknowledges support by the European Community.

References

[1] Mulligan, R.C. (1993) Science 260, 926–932.
[2] Lehrman, S. (1999) Nature 401, 517–518.
[3] Felgner, P.L., Gadek, T.R., Holm, M., Roman, R., Chan, H.W., Wenz, M., Northrop, J.P., Ringold, G.M. and Danielsen, M. (1987) Proc. Natl. Acad. Sci. USA 84, 7413–7417.
[4] Felgner, P.L. and Ringold, G.M. (1989) Nature 337, 387–388.
[5] Felgner, P.L. and Rhodes, G. (1991) Nature 349, 351–352.
[6] Sternberg, B., Sorgi, F.L. and Huang, L. (1994) FEBS Lett. 356, 361–366.
[7] Gustafsson, J., Arvidson, G., Karlsson, G. and Almgren, M. (1995) Biochim. Biophys. Acta 1235, 305–312.
[8] Koltover, I., Salditt, T., Rädler, J.O. and Safinya, C.R. (1998) Science 281, 78–81.
[9] Rädler, J.O., Koltover, I., Salditt, T. and Safinya, C.R. (1997) Science 275, 810–814.
[10] Filion, M.C. and Phillips, N.C. (1997) Biochim. Biophys. Acta 1329, 345–356.
[11] Senior, J.H., Trimble, K.R. and Maskiewiscz, R. (1991) Biochim. Biophys. Acta 1070, 173–179.
[12] Chonn, A., Cullis, P.R. and Devine, D.V. (1991) J. Immunol. 146, 4234–4241.
[13] Malone, R. (1995) Non-viral Genetic Therapeutics: Advances, Challenges and Applications for Self-assembling Systems, IBC's Library Series, Boston, MA.
[14] Diat, O. and Roux, D. (1993) J. Phys. II France 3, 9–14.
[15] Pincet, F., Cribier, S. and Perez, E. (1999) Eur. Phys. J. B 11, 127–130.
[16] Grosberg, A.Y. and Khokhlov, A.R. (1994) Statistical Physics of Macromolecules, AIP, New York.
[17] Franks, N.P. and Lieb, W.R. (1979) J. Mol. Biol. 131, 469–500.
[18] Blaurock, A.E. (1971) J. Mol. Biol. 56, 35–52.
[19] Nallet, F., Roux, D., Quilliet, C., Fabre, P. and Milner, S.T. (1994) J. Phys. II France 4, 1477–1499.